# Optical detection of EPR and electron-nuclear double resonance for substitutional $Mn_{In}^{-}(d^5)$ in InP:Sn

H. J. Sun, R. E. Peale,* and G. D. Watkins
*Department of Physics, Sherman Fairchild Laboratory 161, Lehigh University, Bethlehem, Pennsylvania 18015*
(Received 19 December 1991)

An isotropic optically detected magnetic-resonance (ODMR) peak at $g=1.997$ is found in as-grown Sn-doped InP while monitoring the magnetic circular dichroism (MCD) of an absorption band at ~900 nm. No fine or hyperfine structure is resolved. Optically detected electron-nuclear double resonance (ODENDOR) reveals spectra arising from a central Mn core ($I=\frac{5}{2}$, with isotropic hyperfine interaction $A/h=-166.0\pm0.3$ MHz) and neighboring P and In shells. The pattern and spacings of these lines reveal that the defect is isolated $Mn^{-}(d^5)$, substituting for In, with $S=\frac{5}{2}$. A surprise observation is that the MCD, ODMR, and ODENDOR disappear abruptly when the material is converted to high-resistivity $n$ type by electron irradiation.

## I. INTRODUCTION

Here we report the observation of a defect-related absorption band at ~900 nm in nominally pure $n$-type InP:Sn which we find disappears abruptly upon conversion of the material to high-resistivity $n$ type by 2.5 MeV electron irradiation. The band displays temperature-dependent magnetic circular dichroism (MCD) revealing that the ground state of the defect is paramagnetic. Optical detection of magnetic resonance (ODMR) via the MCD reveals a structureless isotropic resonance at $g=1.997$, providing little information concerning its identification.

In view of the curious Fermi-level dependence near the conduction-band edge, we have therefore also initiated ODENDOR studies (optical detection of electron-nuclear double resonance) to identify the defect. To our surprise, we find that it arises from $Mn_{In}^{-}(d^5)$ and we are faced with having to explain why it disappears in high-resistivity $n$-type material when its acceptor level has been previously established to be at $E_V+0.22$ eV.[1]

This paper is organized as follows. Section II gives experimental details. Section III presents experimental results. Discussions and conclusions are given in Sec. IV, where a tentative model is suggested for the Fermi-level dependence.

## II. EXPERIMENTAL DETAILS

Our 0.4-mm-thick samples were as-grown, single-crystal InP prepared by the liquid-encapsulated Czochralski method, and Sn doped to a concentration of $(1-3)\times10^{16}$ cm$^{-3}$. They were grown at AT&T Bell Laboratory by W. A. Bonner and supplied to us by M. Stavola. Some specimens were irradiated at room temperature with 2.5-MeV electrons to a fluence of $2\times10^{16}$ cm$^{-2}$ or $6\times10^{16}$ cm$^{-2}$.

For the MCD, ODMR, and ODENDOR experiments, the sample was immersed in pumped liquid helium (1.7 K) in an Oxford Instruments SM-4 optical cryostat with a built-in superconducting magnet and quartz windows. The sample was mounted in a 35-GHz $TE_{011}$ microwave cavity designed in the form of concentric rings for optical access.

The excitation source was a 600-W tungsten-halogen lamp. A Jarrel-Ash, Mark X, $\frac{1}{4}$-m monochromator selected wavelength, and colored glass filtered out unwanted orders. A Polaroid HR linear polarizer and Hinds PEM-3 photoelastic modulator produced alternatively left- and right-circularly polarized light at 50.4 kHz. A North Coast liquid-nitrogen-cooled Ge detector collected the transmitted light propagating along the static magnetic field. The output of the detector was synchronously lock-in amplified so that the recorded signal was proportional to the transmission difference between right- and left-circular polarizations.

MCD is defined as the difference in absorption coefficients for left- and right-circularly polarized light.[2] ODMR spectra were obtained by monitoring the change in MCD induced by microwave transitions between Zeeman-split components of the ground state. For the ODENDOR studies, a two-turn coil was installed in the cavity such that its magnetic-field axis was perpendicular to both the static and microwave magnetic fields. The radio frequency was supplied to the coil from a Fluke 6060B frequency synthesizer amplified by an ENI 3100LA solid-state radio-frequency amplifier. The static magnetic field was tuned to the peak of the ODMR resonance, and changes in the ODMR signal intensity were recorded as the radio frequency was swept. The frequency sweep of the synthesizer was computer controlled, and digital signal averaging was performed as necessary.

## III. RESULTS

Figure 1 presents the MCD versus wavelength in as-grown Sn-doped InP. The difference between 1.8- and 0-T spectra is plotted to subtract the field-independent background. Two sharp peaks at 886, 897, and a broad shoulder around 911 nm are found and are indicated by arrows and labeled 1, 2, and 3, respectively. The spectral features in Fig. 1 are reduced by a factor ~7 after elec-

 

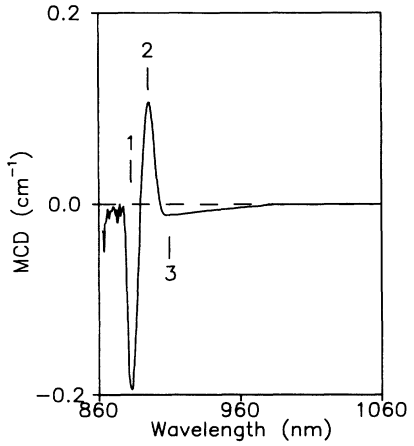


FIG. 1. MCD spectrum of as-grown InP:Sn at $B=1.8$ T and $T=1.7$ K.

tron irradiation with $2\times10^{16}$ $e^-/cm^2$ and are completely absent after $6\times10^{16}$ $e^-/cm^2$. A broad ODMR peak with $g=1.997$ is observed when the wavelength is set to any one of the three MCD peaks.

Figure 2 presents the ODMR spectrum taken with the wavelength set on MCD peak 2. The spectrum was obtained with the magnetic field parallel to a ⟨100⟩ axis of the sample and gives a $g$ value of 1.997 and a linewidth [full width at half maximum (FWHM)] of about 360 G. The single-peak spectrum is isotropic showing no detectable change versus magnetic-field orientation. The line shape is independent of the microwave power and no fine or hyperfine structure is resolved. Figure 2 shows that the line shape is non-Gaussian with a somewhat flatter top. This feature will be analyzed more completely below.

The ODMR spectrum can be fit to the following simple Hamiltonian:

$$H=g\mu_B\mathbf{B}\cdot\mathbf{S}\ . \tag{1}$$

The spin of the defect cannot be determined from the ODMR spectrum alone. Like the MCD in Fig. 1, the ODMR peak of Fig. 2 also decreases with irradiation and is absent after $6\times10^{16}$ $e^-/cm^2$.

Figure 3 presents the ODMR spectrum of the lightly irradiated sample with $2\times10^{16}$ $e^-/cm^2$. New resonances are apparent flanking the reduced intensity $g=1.997$ resonance (central peak). The two new resonances are attributed to an antisite defect $P_{In}$ with $g=1.990\pm0.003$ and a central hyperfine constant $A=(940\pm20)\times10^{-4}$ $cm^{-1}$.[3] After further electron irradiation to a total dose of $6\times10^{16}$ $cm^{-2}$, the antisite resonances increase in intensity and the $g=1.997$ resonance disappears.

It has been established by earlier studies[3,4] that electron irradiation serves to lower the Fermi level of $n$-type InP as deeper levels formed by the irradiation remove carriers from the shallow donors. This can be monitored directly also in our ODMR experiments, the $Q$ of the microwave cavity being poor in the as-grown material, improving with the first irradiation dose, and recovering fully after the $6\times10^{16}$ $e^-/cm^2$ dose. A possible explanation therefore for the disappearance of the $g=1.997$ ODMR signal is that it arises from a defect with a filled energy level close to the conduction-band minimum which becomes depopulated as the Fermi level shifts down in the band gap with electron irradiation. However, we will show below that this simple reasoning can sometimes lead to false conclusions in optical experiments at cryogenic temperatures and it is in conflict with other experimental evidence.

Figure 4 shows an ODENDOR spectrum of as-grown $n$-type InP:Sn obtained with the wavelength fixed at MCD peak 2 and with the magnetic field tuned to the ODMR peak position at 1.25 T. The field was oriented along a ⟨100⟩ axis of the sample. The spectrum was observed only in as-grown or slightly electron-irradiated $n$-type InP:Sn but was absent in the more heavily irradiated samples.

To analyze the ODENDOR spectrum, the following

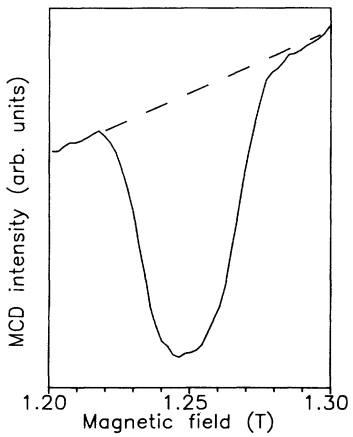


FIG. 2. ODMR spectrum of as-grown InP:Sn at $\lambda=897$ nm, $\nu=35$ GHz, and $T=1.7$ K with $\mathbf{B}\|\langle100\rangle$.

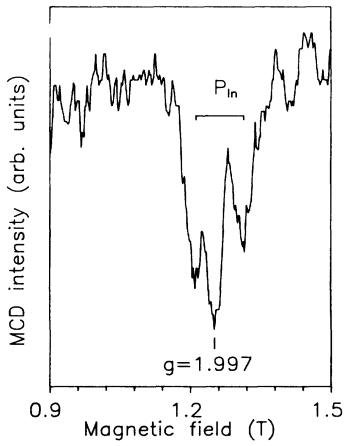


FIG. 3. ODMR spectrum as in Fig. 2 obtained after a small electron-irradiation dose of $2\times10^{16}$ $cm^{-2}$.

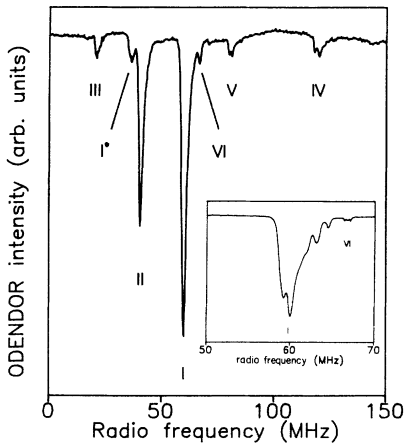


FIG. 4. ODENDOR spectrum obtained with the magnetic field tuned to 1.25 T, the ODMR peak position in Fig. 2. The inset shows spectra I and VI on an expanded scale at reduced rf power.

nuclear-spin Hamiltonian should be added to Eq. (1):

$$H_n = -\sum_i (\mu_i/I_i)\mathbf{B}\cdot\mathbf{I}_i + \sum_i \mathbf{S}\cdot\overleftrightarrow{\mathbf{A}}_i\cdot\mathbf{I}_i + \sum_i \mathbf{I}_i\cdot\overleftrightarrow{\mathbf{Q}}_i\cdot\mathbf{I}\ , \qquad (2)$$

where for the $i$th nucleus, $\overleftrightarrow{\mathbf{A}}_i$ is the hyperfine tensor, $\mu_i$ the nuclear moment, and $\overleftrightarrow{\mathbf{Q}}_i$ the electric quadrupole interaction tensor, which has nonzero matrix elements only for $I_i > \frac{1}{2}$.

A set of negative peaks are evident in Fig. 4 within the 0–130 MHz range. No additional ODENDOR signals were found at higher frequencies up to 200 MHz. The lines are labeled in Fig. 4 by Roman numerals. In order to determine the nuclear species responsible for each line in Fig. 4, the microwave frequency was retuned to shift the ODMR resonance to a new value of the magnetic field. The nuclear gyromagnetic ratio $(\mu_i/I_i)$ was estimated for each ODENDOR line from its center frequency shift for a change in the magnetic field. This allowed us to identify all but one of the lines with specific nuclear species assuming the first-order relation $d\nu_i/dB = \pm\mu_i/I_i h$. Signals I, I*, II, and III arise from nearby $^{115}$In nuclei ($d\nu_i/dB = +9.2\pm0.5$ MHz/T for I, II, and III and $-9.2\pm0.5$ MHz/T for I*). Signals IV and V are identified with $^{31}$P ($d\nu_i/dB = +17.2\pm0.5$ MHz/T). The value for signal VI was $d\nu_i/dB = -8.0\pm0.5$ MHz/T. The identification of this nucleus will be discussed in more detail below.

The three strong In lines I, II, III in the ODENDOR spectrum are almost equally spaced. Each of these signals shows a similar closely spaced satellite structure, shown on an expanded scale for I in the inset of Fig. 4, when the rf power is reduced. The spectrum can be followed over the range $\mathbf{B}\|\langle 100\rangle \pm 72°$ in a $\{100\}$ plane and also with weaker signal at 90° ($\mathbf{B}\|\langle 110\rangle$), the light entering the thin edge of the wafer crystal. The angular dependence of the In lines is currently under investigation. Although the analysis is not complete, the general pattern of the angular dependence is similar for the I, II, and III lines and appears consistent with $C_{1h}$ symmetry.

These observations provide an important clue as to the origin of the lines and their correct analysis. This can be seen as follows: Consider for the sake of illustration the first-order solution for the ODENDOR frequencies in the absence of anisotropy in $A_i$ and quadrupole interactions,

$$h\nu(M, m_i \leftrightarrow m_i - 1) = |A_i M - (\mu_i/I_i)B| \ . \qquad (3)$$

For each nucleus, there are $2M+1$ transitions predicted. Recognizing this, we note that peaks I, II, III, and I* can be fit accurately with $A_i/h = +19.2\pm0.3$ MHz if they arise from the $M = -\frac{5}{2}, -\frac{3}{2}, -\frac{1}{2}$, and $+\frac{5}{2}$ states, respectively, of an electronic $S = \frac{5}{2}$ system. (The $M = +\frac{3}{2}$ resonance would be at $\sim 37$ MHz and we note a weak resonance at this frequency also. The $M = +\frac{1}{2}$ would be at $\sim 1$ MHz and would probably be difficult to detect.) The decreasing intensity for I$\rightarrow$II$\rightarrow$III, etc., results from the large Zeeman-Boltzmann distribution difference at $T \sim 1.7$ K, and the change in sign of $M$ for I* explains its opposite field shift. Taken together, this provides unambiguous proof that the defect has $S = \frac{5}{2}$ and that the I, II, III, and I* resonances all arise from In nuclei in a single shell surrounding the defect.

The intensities of the $P$ lines are considerably weaker than the In lines, and they could only be followed for $\mathbf{B}\|\langle 100\rangle \pm 20°$. Analysis reveals that line V arises from the $M = -\frac{3}{2}$ state and line IV arises from the $M = -\frac{5}{2}$ state, respectively, with $(A_P/h)_{\langle 100\rangle} = +39.2\pm0.3$ MHz. The $M = -\frac{1}{2}$ transition is not observed in Fig. 4 since it is obscured by the strong signal II, but studies under high resolution at low rf power show evidence of it. The other $M$ transitions are presumably too weak to be observed. As seen in Fig. 4, each P line is split into two lines with separations for line IV and V of 2 and 1.2 MHz, respectively. [The value for $(A_P/h)_{\langle 100\rangle}$ above was determined from the center position between the two lines.] The origin of this splitting is currently under investigation. From the angular dependence of the P lines, the hyperfine parameters for the P shell appear consistent with $C_{3v}$-$\langle 111\rangle$ symmetry with $A_{P\|}/h \sim +41$ MHz and $A_{P\perp}/h \sim +38$ MHz.

Next, we address the origin of signal VI, which is observed with a field shift $d\nu_i/dB = -8.0\pm0.5$ MHz/T. Although it has been concluded that the defect has $S = \frac{5}{2}$, we still do not know its identity. It is surprising at first glance that the hyperfine interactions of the P and In shell are so small since the FWHM linewidth of the ODMR resonance is 360 G while the hyperfine interactions found for the In and P shells in ODENDOR are only $\sim 20$ and 40 MHz, which are too small to account for the linewidth of the ODMR spectrum. For example, simulation of the line shape for four nearest P and 12 next-nearest In neighbors with these hyperfine interactions gives a FWHM width of only 170 G (see the discussion in the next section and Fig. 6). We conclude that an important additional large hyperfine interaction must also exist, presumably related to signal VI.

With this in mind, we explore the possibility that the VI signal results from the $M = -\frac{1}{2}$ state. With $d\nu_i/dB = -8$ MHz/T, Eq. (3) indicates $A_i/h \sim \mp 140$ MHz and $\mu_i/I_i h \sim \pm 8$ MHz/T. Under these conditions,

only one transition is expected as observed, the stronger $M=-\frac{3}{2}$ and $M=-\frac{5}{2}$ transitions predicted at $\sim 220$ and 360 MHz, respectively, out of range for our radio-frequency generator. For this large hyperfine interaction, second-order corrections, $\sim A^2/g\mu_B Bh$, are sufficiently important that they must be included in the analysis of the ODENDOR spectrum. Adding this term to Eq. (3), the transition frequencies become

$$h\nu_i(M, m_i \leftrightarrow m_i-1)=|A_i M-(\mu_i/I_i)B-(A_i^2/2g\mu_B B)[S(S+1)-M^2+(2m_i-1)M]| \ . \tag{4}$$

For $M=-\frac{1}{2}$, and with $|A_i/2|>|(\mu_i/I_i)B|$, the change of resonance frequency $\nu_i$ versus the change of magnetic field is given, to second order, by

$$\frac{d(h\nu_i)}{dB}\cong\frac{A_i}{|A_i|}\{\mu_i/I_i-(A_i^2/2g\mu_B B^2) \times[\tfrac{17}{2}-(2m_i-1)M]\} \ . \tag{5}$$

Equation (4) predicts $2I$ equally spaced lines separated by $A^2/2g\mu_B Bh$ for the $m_i \rightarrow m_{i-1}$ transitions of a nucleus with spin $I$. Under the higher resolution obtained in the low rf power studies (see inset in Fig. 4), the VI signal is indeed found to be made up of five equally spaced lines with $\sim 0.35$ MHz separation, where the relative amplitudes vary depending upon where in the inhomogeneously broadened ODMR line the magnetic field is tuned. These results are shown in Fig. 5. This establishes that the nuclear spin is $I=\frac{5}{2}$.

Angular dependence studies of these ODENDOR lines reveal that they remain unchanged ($\pm 0.1$ MHz) over the $\mathbf{B}\|\langle 100\rangle \pm 57°$ studied. There is, therefore, no evidence of a quadrupole interaction or anisotropy of the magnetic hyperfine interaction.

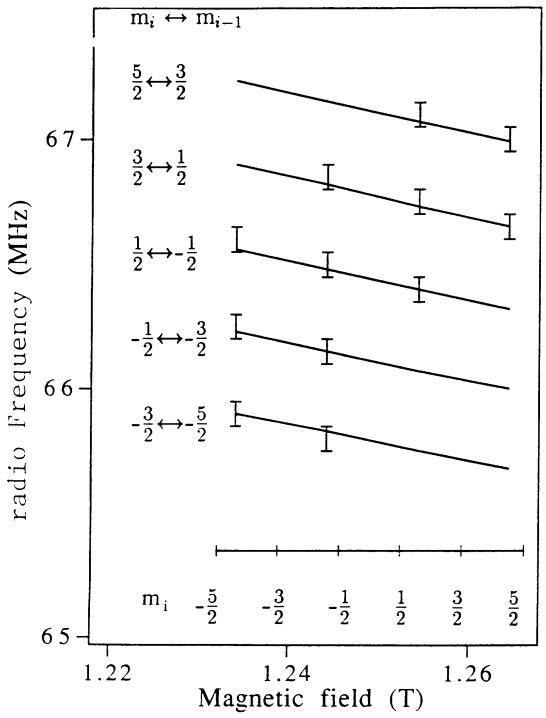


FIG. 5. Resolved transitions of ODENDOR line VI for $B$ at several points within the ODMR linewidth (solid lines, theory for $I=\frac{5}{2}$).

## IV. DISCUSSION AND CONCLUSIONS

We have established the following about the defect: In the ground state of the optical transition, the defect has $S=\frac{5}{2}$ and the impurity at the core has nuclear spin $I=\frac{5}{2}$. The isotropy of the ODMR signal with no evidence of lower-symmetry fine structure, and the absence of hyperfine anisotropy or quadrupole interaction for the central impurity, reveal that the defect has overall $T_d$ symmetry. Simultaneous solution of Eqs. (4) and (5) for the observed central impurity $m_i=+\frac{1}{2}\rightarrow-\frac{1}{2}$ ODENDOR frequency ($66.4\pm 0.1$ MHz) and its shift versus $B$ ($-8.0\mp 0.5$ MHz/T) gives two possibilities: $A_i/h=-166\pm 2$ MHz, $\mu_i/I_i h=+10.7\pm 0.6$ MHz/T or $A_i/h=+153\pm 2$ MHz, $\mu_i/I_i h=-5.7\pm 0.5$ MHz/T. There are only two candidates in the Periodic Table, $^{27}$Al ($+11.1$ MHz/T) and $^{55}$Mn ($+10.56$ MHz/T). Only the second with its inner $d^5$ shell can account for $S=\frac{5}{2}$.

We conclude therefore that the central impurity is manganese. ODENDOR of a single shell each of P and In surrounding the central manganese impurity has been observed. The symmetry of their spectra are consistent with the first-neighbor P and second-neighbor In shells surrounding substitutional Mn on an In site, i.e., $Mn_{In}$. (Further evidence that the Mn impurity is substitutional rather than in an interstitial $T_d$ site comes from comparison to GaAs and GaP, where magnetic resonance has been reported for Mn in both sites. The interstitial site in these materials displays a much larger hyperfine interaction ($\sim 266$ MHz),[5] while the values for the substitutional site are very close to our result here for InP [162.2 MHz for GaAs (Refs. 5 and 6), 159.2 MHz for GaP (Ref. 7)].)

The ODMR and ODENDOR results are summarized in Table I. With the identification of the central nucleus as $^{55}$Mn ($\mu/Ih=+10.56$ MHz/T), a match to the five manganese $M=-\frac{1}{2}$ ODENDOR transitions in Fig. 5 was performed using exact diagonalization of Eq. (2) giving $A_{Mn}/h=-166.0\pm 0.3$ MHz. The results are plotted as the solid lines in Fig. 5 and the agreement is excellent. With these values of the hyperfine interactions, the line shape of the ODMR signal has been calculated and the result is shown in Fig. 6. The solid lines present the line shapes of the computer simulation. The six equivalent curves represent the calculated line shape resulting from

TABLE I. Hyperfine parameters for $Mn_{In}^{-}(d^5)$ in InP ($g=1.997$, $S=\frac{5}{2}$).

| Nucleus (site) | $I$ | $(A_i)_{\langle 100\rangle}$ (MHz) | $(A_\parallel)_i$ (MHz) | $(A_\perp)_i$ (MHz) |
|---|---|---|---|---|
| $^{55}$Mn (core) | $\frac{5}{2}$ | $-166.0\pm0.3$ | | |
| $^{31}$P (1$nn$) | $\frac{1}{2}$ | $+39.2\pm0.3$ | $\sim42$ | $\sim38$ |
| $^{115}$In (2$nn$) | $\frac{9}{2}$ | $+19.2\pm0.3$ | | |

the four nearest P and twelve next-nearest In neighbors alone, but centered on the six hyperfine line positions for the central $I=\frac{5}{2}$ manganese nucleus. The ODMR line shape consists of the sum of these six curves. The dashed line with crosses presents the experimental result. The agreement is excellent.

We conclude therefore that the MCD absorption band and its related ODMR and ODENDOR spectra arise from isolated substitutional $Mn_{In}^{-}(d^5)$ as an unintentional impurity in the material. Of course, we might have suspected manganese at the outset because of the somewhat flat-topped character of the ODMR, and certainly as soon as the ODENDOR revealed $S=\frac{5}{2}$. Indeed, it has been previously established that manganese introduces a single acceptor level ($-/0$) at $E_V+0.22$ eV.[1] No other level is believed to be in the gap so that in the $n$-type material, we expect the EPR-active $Mn^{-}(d^5)$ state. However, it was not expected therefore to disappear abruptly as soon as carriers were removed from the shallow donor state by irradiation. It has been previously demonstrated that even after prolonged irradiation the material remains $n$ type (high resistivity) and the stable charge state should therefore remain $Mn^{-}$.[3,4]

Having now established that it is indeed $Mn_{In}^{-}$, we must consider why it disappears so quickly upon electron irradiation. One explanation might be that the isolated substitutional Mn center combines with defects produced by electron irradiation to make a new complex center not observed by MCD or ODMR. This, or course, is possible but perhaps unlikely at these low irradiation doses.

An alternative explanation, which is consistent with the accepted level assignment, is given in Fig. 7. In this model, the observed MCD is found in the photoionization band of $Mn^{-}$ from its acceptor ($-10$) level. For as-grown InP, the paramagnetic charge state $Mn^{-}$ should be quickly repopulated via the Sn shallow extended donor states [with the energy level being at $\sim E_C-7.4$ meV (Refs. 8 and 9)]. Electron irradiation creates highly localized deep levels in the band gap. The electrons photoionized from the Mn acceptor level can then become trapped at the deep levels, and hence the $Mn^{-}$ state could be rapidly depopulated by the excitation light and the MCD would disappear. We suggest that this is the more likely explanation, arguments involving the Fermi-level position being dangerous at cryogenic temperatures where electronic equilibration cannot occur. (A similar explanation has been called upon to explain the existence of MCD and ODMR of isolated antisites in $p$-type InP where the equilibrium state should be nonparamagnetic $P_{In}^{2+}$.[3])

The spin-Hamiltonian parameters that we have determined match well those deduced from previous EPR (Ref. 10) and ODMR photoluminescence (PL) studies[11] in intentionally Mn-doped InP. It is interesting to note, however, that in both of these previous studies, and for somewhat different reasons, the authors concluded that the signals arose from *neutral* manganese and that the observed $d^5$ resonance results therefore from a $d^5$ $Mn^{-}$ core plus a weakly coupled bound hole. (For the EPR studies, the material was $p$ type and it was argued that the strong intensity of the resonance ruled out its coming from $Mn^{-}$.[10] For the PL-ODMR studies, it was argued that the luminescence originated from shallow donor to neutral manganese acceptor recombination.[11]) We now know, however, from studies in GaAs:Mn,[12,13] where the neutral state has been established to be $Mn^{-}+h^{+}$, that the EPR signal is very much different, arising from the $J=1$ manifold of the coupled $S=\frac{5}{2}$ $d^5$ core plus the $J=\frac{3}{2}$ hole. [In InP, the hole binding (0.22 eV) is even greater than that in GaAs (0.11 eV) and the coupling of the hole should be even greater.] It appears, therefore, that the $Mn^{0}$ interpretation of these authors must be ruled out. Instead, they must have been detecting $Mn^{-}(d^5)$, the same as we have observed. Again, therefore, as in our case, the $Mn^{-}(d^5)$ resonance appears to be showing up in ways contrary to expectations in InP. The explanation in the case of the EPR studies could be that compensation

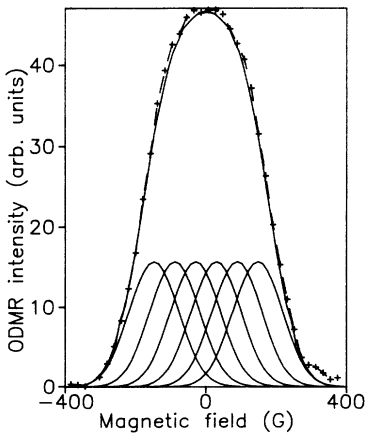


FIG. 6. Comparison of the experimental ODMR signal (dashed line) with a simulation (solid lines) using the hyperfine parameters given in Table I.

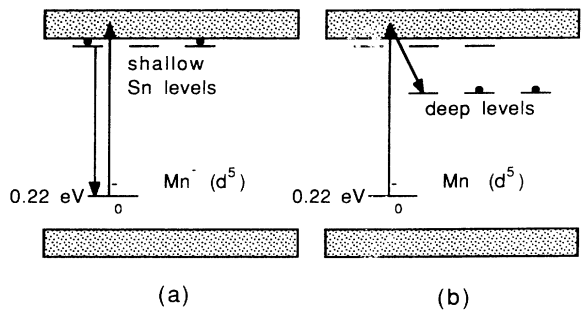


FIG. 7. Model for how $e$ irradiation kills $Mn^{-}(d^5)$ MCD and ODMR. (a) As-grown $n$ type; (b) $e$ irradiated but still $n$ type.

by residual donors was underestimated, but in the case of the PL-ODMR studies the explanation is less clear. Perhaps spin memory in the pumping cycle[14] served to reveal ODMR in the ground $Mn^{-}(d^5)$ state.

Finally, we mention a remarkable and unusual feature of the ODENDOR signals. Figure 8 reveals the effect of the microwave (ODMR) and the rf (ODENDOR) on the intensity of MCD peaks 1, 2, and 3. The solid curve (a) shows the MCD measured with magnetic field off of the ODMR peak and rf power off. The dotted curve (b) was measured with the magnetic field tuned to the ODMR peak, but with rf power still off. The dashed curve (c) was measured with magnetic field on the ODMR peak and radio frequency tuned to 60 MHz, the position of ODENDOR peak I. The signs of the intensity change of the MCD spectra are consistent with the signs of the ODMR and ODENDOR peaks. Clearly, the change of the MCD peak intensity induced by the ODENDOR rf transitions is about twice as large as the change induced by the ODMR microwave transitions. The intensity of the ODENDOR signal is 200% of the ODMR signal! This is most unusual. ODENDOR signals have been occasionally reported to be comparable to the ODMR signals, but this is the first reported case to our knowledge where the ODENDOR signal exceeds that of the ODMR. One reason is clearly the fact that with the In $I=\frac{9}{2}$ nucleus, nine $\Delta m=\pm 1$ transitions all superpose for $\mathbf{B}\|\langle 100\rangle$ allowing nine separate nonsaturated spin packets in the inhomogeneously broadened ODMR line to be fed into the saturated one.

In conclusion, an isotropic ODMR peak, with $g$ value equal to $1.997\pm0.002$ and linewidth equal to $360\pm10$ G, is found in as-grown Sn-doped InP while monitoring the magnetic circular dichroism (MCD) at ~900 nm. No fine or hyperfine structure is resolved in the ODMR spectrum. The pattern and spacing of the peaks of the ODENDOR spectrum uniquely identify the defect as having $S=\frac{5}{2}$ and a central nucleus with $I=\frac{5}{2}$. The defect is identified to be an isolated substitutional $Mn_{In}^{-}$ center with tetrahedral symmetry. The hyperfine interactions arising from the Mn core and the first P and In shells have been identified by ODENDOR.

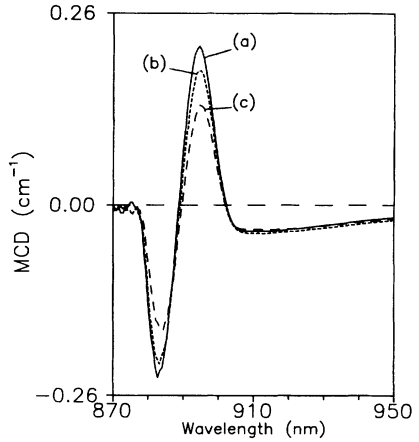


FIG. 8. (a) MCD spectrum without microwaves and rf. (b) MCD with microwaves tuned to ODMR. (c) MCD with microwaves tuned to ODMR and rf tuned to ODENDOR peak I.

## ACKNOWLEDGMENT

This research was supported by the National Science Foundation under Grant No. DMR-89-02572.

*Present address: Department of Physics, University of Central Florida, Orlando, FL 32816-0385.

[1]B. C. Clerjaud, J. Phys. C **18**, 3615 (1985).
[2]D. Y. Jeon, H. P. Gislason, J. F. Donegan, and G. D. Watkins, Phys. Rev. B **36**, 1324 (1987).
[3]H. P. Gislason, H. J. Sun, F. C. Rong, and G. D. Watkins, in *The Physics of Semiconductors, Vol. 1*, edited by E. M. Anastassakis and J. D. Joannopoulous (World Scientific, Singapore, 1990), p. 666.
[4]K. Ando, A. Katsui, D. Y. Jeon, G. D. Watkins, and H. P. Gislason, Mater. Sci. Forum **38-41**, 761 (1989).
[5]S. J. C. H. M. Van Gisbergen, M. Godlewski, T. Gregorkiewicz, and C. A. J. Ammerlaan, Phys. Rev. B **44**, 3012 (1991).
[6]V. F. Masterov, S. B. Mikhrin, B. E. Samorukov, and K. F. Shtel'makh, Fiz. Tekh. Poluprovodn. **19**, 2093 (1985) [Sov. Phys. Semicond. **19**, 1291 (1985)].
[7]P. Van Engelen and S. G. Sie, Solid State Commun. **30**, 515 (1979).
[8]P. J. Dean, M. S. Skolnick, and L. L. Taylor, J. Appl. Phys. **55**, 957 (1984).
[9]M. S. Skolnick, P. J. Dean, L. L. Taylor, and D. A. Anderson, Appl. Phys. Lett. **44**, 881 (1984).
[10]V. F. Masterov, Yu. V. Mal'tsev, and V. K. Sobolevskii, Fiz. Tekh. Poluprovodn. **15**, 2127 (1981) [Sov. Phys. Semicond. **15**, 1235 (1981)].
[11]Yan Dawei, B. C. Cavenett, and M. S. Skolnick, J. Phys. C **16**, L647 (1983).
[12]J. Schneider, U. Kaufmann, W. Wilkening, and M. Baeumler, Phys. Rev. Lett. **59**, 240 (1987).
[13]M. Baeumler, B. K. Meyer, U. Kaufmann, and J. Schneider, Mater. Sci. Forum **38-41**, 797 (1989).
[14]L. F. Mollenauer and S. Pan, Phys. Rev. B **6**, 772 (1972).

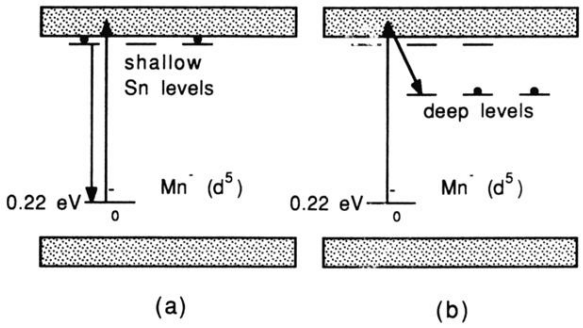


FIG. 7. Model for how $e$ irradiation kills $Mn^{-}(d^5)$ MCD and ODMR. (a) As-grown $n$ type; (b) $e$ irradiated but still $n$ type.